DSC-investigation of ultra thin sheet of NiTi Shape Memory Alloy

Farwa Shaukat[1], Muhammad Arshad Javid[1], Muhammad Irfan[1], M.Saifullah. Awan[2]

1. Department of Basic Sciences and Humanities, University of Engineering and Technology Taxila.47050
2. Nanoscience and Technology Department, National Center for Physics Islamabad, Pakistan

∗ **Corresponding Author:** Email: sssawan@gmail.com

Abstract

The objective of this work was to develop and investigate the 3d-transition metal NiTi shape memory alloy for its transformation temperatures. The alloy was prepared by using chips of metallic Ni and Ti in the vacuum arc melting furnace. Melting was carried out under the protective atmosphere of Argon gas. An ultra-thin sheet (0.3mm) was prepared by cold-rolling the alloy. An intensive cold rolled sheet of NiTi was inspected for structural, microstructure, elemental composition and thermal cyclic behavior using XRD, FE-SEM, EDX and DSC studies respectively. The alloy sheet sample was annealed in the temperature range of (300-900)℃ for 20 minutes. DSC scan was carried out in the temperature range between (200 ℃→ -60 ℃→ 200 ℃ for as rolled, annealed and for thermal cycling. In the early stage of annealing, highly diminished martensitic and austenitic peaks in the DSC-thermo gram evidenced that the alloy microstructure structure was under high stress. An optical micrograph revealed the rolled structure of the alloy sheet. DSC examinations further revealed that the cyclic and phase-transformation behaviour of the alloy was significantly influenced by heat treatment. As a result of annealing, the transformation temperatures of austenite and martensite have shifted from 37.922 ℃ to 61.344 ℃ and from 53.453 ℃ to 72.322 ℃ respectively. The hysteresis between martensite and austenite decreases by 10.978 ℃ as the annealing temperatures increase. Stable behaviour of transformation temperature is observed after annealing at 650 ℃ and above. No change in the transformation temperatures was observed during thermal cycling. This study concludes that the variation in the transformation temperatures is the result of stress relief of martensitic plates during annealing treatment. The stable behaviour of transformations temperatures during annealing as well as during thermal cycling is due to dislocation tangling and precipitation.

Key Words: Martensitic, hysteresis, ultra-thin sheet, thermal cycling, stress relieving, tangling, cold rolling

1. Introduction

Shape Memory Alloys are a subset of blessed materials that have a memory and a highly superelastic character. A MEMORY is something that is rememorized/restored [1- 2]. When a smart material undergoes some deformation and is exposed to a suitable temperature, it magically memorizes its original shape for a prescribed period of time. Whereas super-elasticity is defined as shape recovery after significant deformation upon unloading. Shape memory effects are a common result of shape memory alloys, and as a result of this exceptional effect, shape memory alloys demonstrate a glow to researchers and scientists [4]. These smart alloys have an exclusive characteristic which is responsible for their shape memorization, i.e., a unique phase transformation of their crystallographic structure upon heating and cooling. 3d transition metals, such as the nickel-titanium alloy NiTi, are examples of smart alloys that exhibit shape memory [5]. NiTi-alloys exhibit two-stable phases. The high temperature phase is known as Austenite, and the low temperature phase is known as Martensite. The Base Centered Cubic structure (B2) is the Austenite crystal structure, named after the English physicist, Charles Austen. The crystal structure of martensite is a monoclinic site crystal that has two stable, twinned martensite (B19') and a detwinned martensite (B19), the Martensite phase name subsequent to the German Physicist Adolf Martens'[5-6]. The Martensite crystal structure forms a twinned symmetric structure. Twinning of martensite refers to a structure like a mirror image in which each layer is parted from the other layer through a twinning boundary. The twinned boundaries of a martensite structure have a distinctive ability to undergo some degree of deformation without contravention of atomic [5]. While the Austenite phase is a stronger phase and is not easily deformable, when we apply some mechanical force to the twinned martensite by the application of external mechanical force, the twinned martensite crystal structure switches its orientation to deformed martensite through the movement of the twinned boundaries. The detwinned martensite completely transformed into

the long-range order structure of austenite after heating the alloy to a higher temperature [4, 5, and 6]. The mechanism of the shape memory effect is depicted in the figures below.

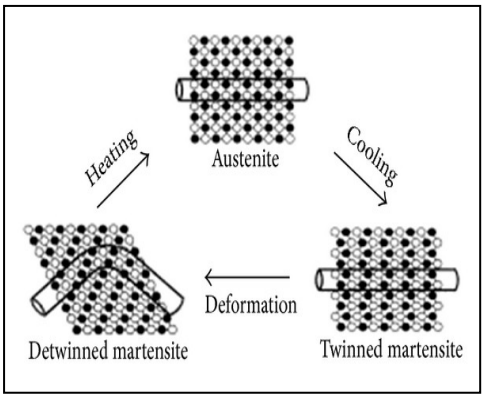

Fig. 1: Phase transformation behaviour in NiTi-alloy

Phase transformations of austenite to martensite and from martensite to austenite proceed at different temperature values. The difference in transformation temperatures between heating and cooling creates a hysterical loop with four transition temperatures. Martenesite starts are represented by M_s and martensite finishes are represented by M_f, and Austenite starts and finishes are represented by A_s and A_f, respectively [8]. Figure (2) shows the thermal hysteria loop.

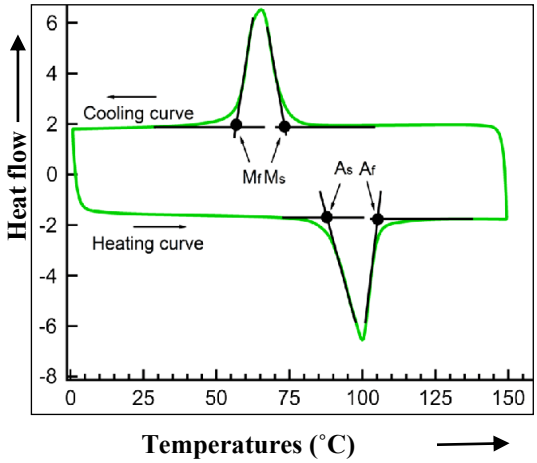

Fig. 2: Hysterics associated with transformation temperatures

The deformed shape memory alloy retains its memorized shape when heated to an austenite finish (A_f), and when cooled, reverse transformation occurs, with the austenite phase beginning to twinned martensite phase at Martensite finish temperature. Shape memory alloy forms a complete cycle between deformed and original shape. For the shape memory phenomena, the development of a twinned structure (B19') during reverse transformation is essential. Along with these two phases, an intermediate phase known as the intermediate R-phase may occur [15]. The crystal structure of this phase is rhombohedral. In general, shape memory alloys are divided into three types: one-way shape memory alloys, two-way shape memory alloys, and all-around shape memory alloys. In one way, the shape memory alloy memorizes its original shape only upon heating and external mechanical strength is required to deform the twinned structure of the SMA alloy. Two-way shape memory alloys remember their original shape both when heated and when cooled, requiring no external mechanical strength. The all-around type of shape memory alloy is based on the concentration of Ni. Alloys with a Ni concentration greater than Ti will have a strange memory effect, similar to the two-way shape memory effect, but extreme deformation is required for "all-around" shape memory alloys. When the temperature of an alloy falls below the transition temperature, it will involuntarily turn around in its shape in the opposite direction of the deformation; when the temperature of the alloy rises above the transition temperature, it will revert to its memorized shape. All the types of shape memory alloys are based on a training mechanism [4]. Besides the shape memory phenomenon, NiTi exhibits auxiliary good properties like corrosion resistance, high fatigue strength, and due to the light weight and self accommodative nature of NiTi, it shows flicker for low and high temperature applications like aerospace, aircraft, aeronautical engineering, and also for automobiles. NiTi with an elemental composition near 50, 50 shows great importance for medical applications. Transformation temperatures of near equiatomic concentration of Ni and Ti are extremely ordinary at body transformation temperatures, which make Nitinol highly suitable for biomedical applications, e.g. heart stents, orthopedic operation treatment staples, rods, as a bone spacer, and also for orthodontics. NiTi with different compositions is a spark for different fields of applications [3-4-8]. Because of the high melting point of Ti and also its low viscosity, NiTi preparation is a complex procedure. The molten form of Ni, on the other hand, is extremely reactive. For melting and casting the NiTi-shape memory alloy, the Vacuum Arc melting furnace is the best choice [10]. Holding on to the transformation temperatures and to the dislocations/crystal faults are extremely important for the shape recovery phenomenon. In this regard, heating treatments and mechanical work are

critical for achieving the desired properties as well as the best performance of shape memory alloys. Cold rolling is the best mechanical process for achieving the desired properties [8]. Solution treatment, thermal cycling, and annealing, on the other hand, are examples of heating treatments that all contribute to the stability of NiTi transformation temperatures [11-14]. The objective of this work was to develop and investigate the 3d-transition metal NiTi shape memory alloy. DSC measurements were conducted on two kinds of SMA specimens, including as-received and as-annealed conditions. There are many methods for examining the behaviour of crystalline phase transformations. According to a study of the literature, differential scanning calorimetry (DSC) is the ordinary and practical test technique for extracting thermal properties from various SMAs. Obviously, like with any technique, it has a number of benefits and drawbacks [12]. The DSC method generates a thermo gram with distinct peaks when heat enters or leaves a piece of the alloy throughout its phase transitions [13]. Thus, the martensite to austenite transition in SMAs is an endothermic (heat-absorbing) process. On the other hand, the transformation from austenite to martensite is an exothermic reaction. The area under the peaks on calorimetric thermo grams shows the energy of transformation. The crucial transition temperatures may also be calculated using these peaks. Through DSC results, we examined how heating treatment annealing and thermal cycling contribute to the stability of transformation temperatures of solution treated NiTi-alloy with intense cold rolling [12, 13].

2. Experimental Procedure

2.1 Melting and Casting

Melting and casting of NiTi is a very multifaceted process because of its high melting point, low viscous nature, and its affinity for oxidation, especially at high temperatures. In molten form, Ni, on the other hand, is extremely reactive. To make matters easier, the Vacuum Arc re-melting furnace, in particular, is the best choice for melting Ni and Ti. As a result, a Vacuum Arc melting furnace was used to melt NiTi. Metallic chips of Ni and Ti were placed on the Cu hearth. The Ti chips are covered with the N_i piece in order to avoid oxidation of the T_i during melting. The furnace was sealed and Argon gas was filled three times to remove the oxygen content from the furnace chamber. Finally, the A_r was filled and melting was performed under the dynamic flow of the A_r. The NiTi alloy was re-melted four times in order to ensure the homogeneity of the ingot. The alloy was completely homogenized and solidified into an ingot before being cooled under Ar flow. Later, small chips of the NiTi alloy were obtained by a wire cutting machine. A homogenized NiTi chip was subjected to solution treatment in an inert atmosphere under Ar flow at 1000˚C for 2 hours, in order to dissolve any essentials that were captured in the NiTi ingot during melting and casting.

2.2 Plastic Deformation

The Strip of Ni50.24Ti49.86 was deformed in a Martensitic phase in a Duo Rolling Mill. After each step of cold rolling, annealing the deformed strip and then abruptly dipping into a bath of liquid nitrogen improves the capability of further deformation. An intense cold rolled sheet with a thickness of 0.27mm was meticulously spark-cut into square-shaped pieces of about 2x2 mm in size. The specimen of the alloy sheet sample was annealed in the temperature range of (350˚C-750 ˚C) for 20 minutes.

2.3 Heating Treatments for DSC

The Alloy sheet sample was annealed for 20 minutes in an electric muffle furnace (in air) in the temperature range of (350-900)˚C, and then free air-cooled to room temperature. The temperature of the furnace was kept within a 5°C range.

2.4 Characterization Techniques

XRD (Bruker D8 Advance) was used to analyze the phase of NiTi alloy (working at…. Kv, ….mA, λ = 1.54056Å) in the (20-90˚) 2θ range. A scanning electron microscope (FEI QUANTA 450) equipped with EDS detector was used for the determination of elemental composition. The weight percent and atomic percent were also supported by the phase diagram of NiTi. All the transformation temperatures are studied by using differential scanning calorimetry (Mettler Toledo Dsc1).

2.5 DSC measurements

Thermal experiments were performed on the as-received material and specimens following heat treatment at different annealing temperatures to record changes in phase transition behaviors. The DSC measurements were taken within 24 hours of the annealing process. A Mettler Toledo DSC1 was utilized to collect thermal data, and liquid nitrogen was employed as a cooling agent. An indium reference standard was used to calibrate the energy flow and temperature. Thermal cycling

was carried out in the temperature range between (200˚C-60˚C-200˚C). 10K/min is the scanning rate which is held constant throughout the thermal cycling. According to our previous laboratory experiments, a maximum temperature of +200°C was obtained during calorimetric heating, which was found to be much higher than the temperature required to achieve a completely austenite condition for each of the specimens under consideration. Additionally, cooling to -60°C was determined to be below the temperature at which the transition to martensite was stopped, indicating that it was sufficient. Specifically, the following temperature regimes were applied to each specimen: rapid heating from room temperature to +200°C, followed by chilling to about -60°C at a steady cooling rate (10K/min), and lastly, rapid heating from room temperature to +200°C at the same rate.

3. Result and discussions

The as cast and rolled sheet of NiTi alloy was investigated for structural, micro structural, elemental and thermal analysis.

3.1 X-Ray Diffraction

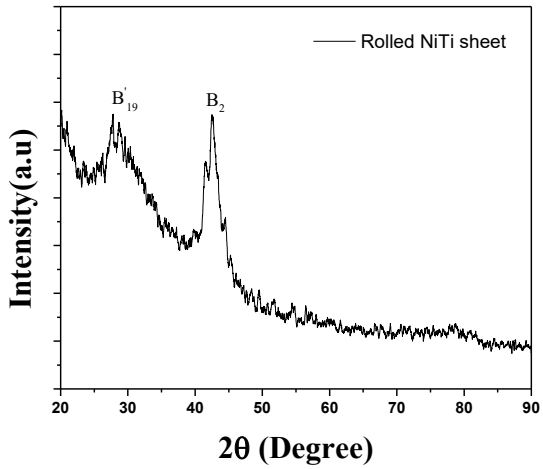

Fig. 3: XRD pattern of the rolled sheet of NiTi

Figure 8 illustrates the findings obtained from rolled sheet of NiTi using the Broker D8 advance machine. It is observed from the above graph that the rolled material comprises two phases: B2 [9] and B19′. Due to intensive cold rolling the material under goes fine crystalline plate like structure, this is evidenced by the presence of broad peaks in the XRD pattern. Diffraction peaks have a greater full width at half maximum (FWHM) for materials that have undergone more deformation [9].

3.2 Scanning Electron Microscopy

Field emission scanning electron microscopy equipped with an EDX detector was used to examine the chemical composition of the NiTi alloy. Figure-4 selected area image used for EDS analysis. Figure-5 is the EDS spectrum of the NiTi alloy, which confirms the elemental composition as shown in Table-1. The Phase diagram also provides the same evidence of elemental composition.

Fig. 4: SEM micrograph sheet of NiTi for EDS analysis

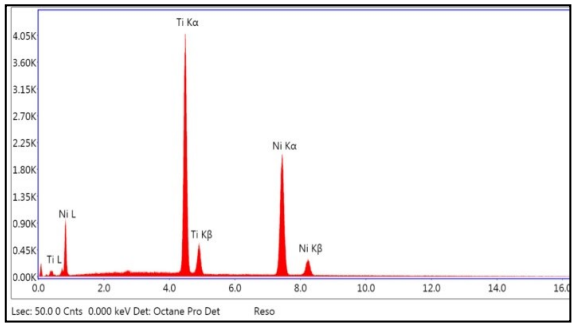

Fig. 5: EDS spectrum of as cast NiTi alloy

Table 1: Atomic and weight% of Ni and Ti

Elements	Shell	Atomic%	Weight%
N_i	K	50.14	44.79
T_i	k	49.86	55.21

3.3 Differential Scanning Calorimetry

NiTi alloy sheet was investigated for thermal signatures using DSC measurements. Transformation temperatures were determined by

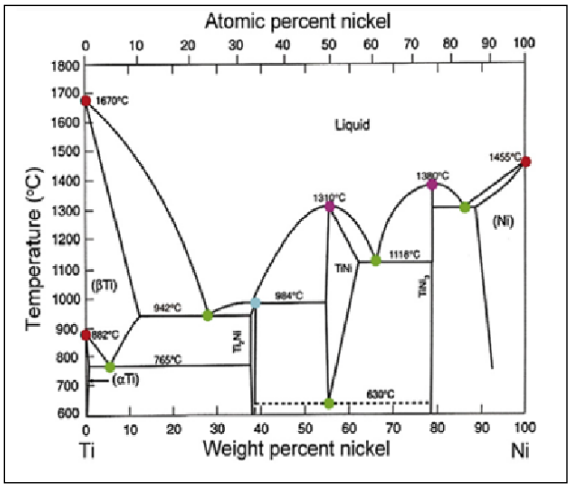

Fig. 6: Phase diagram of NiTi-alloy [7]

thermally cycled the sample from -60 ˚C to 200C and then from -60˚C to 200˚C. Samples were scanned with a heating and cooling rate of 10C/min under inert Ar atmosphere. Arrows indicate the heating and cooling cycle direction. Alloy sheet was annealed in the temperature range of (300˚C-900˚C) in the muffle furnace. Each time sample was heat treated for 20 minutes in air and air cooled to room temperature. The DSC thermo grams of as rolled and annealed samples are discussed in this section.

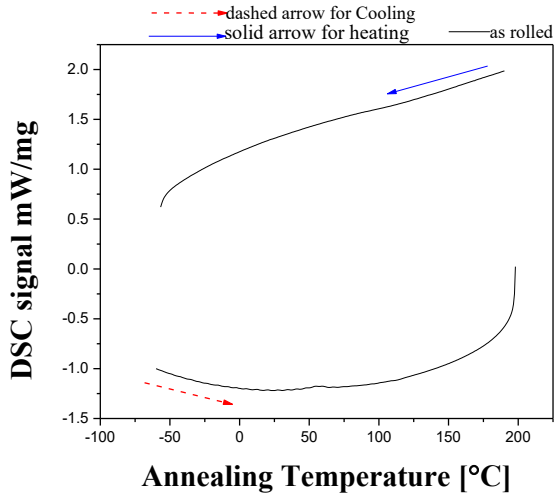

Fig. 7: As-received Ni-Ti alloy's DSC cooling and heating curves

Fig.7 illustrates the phase transformation of rolled NiTi alloy sheet. As shown in the figure, cooling the specimen from +200˚C to -60˚C followed by heating from -60˚C to 200˚C caused no exothermic or endothermic peaks. The result reveals that dislocation and both the phases of NiTi are under high mechanical stress in rolled sheet sample.

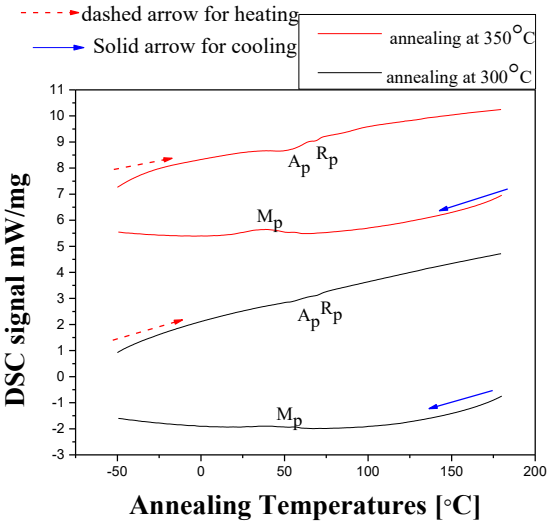

Fig. 8: DSC cooling and heating curves of the Ni-Ti alloy annealed at 300°and at 350˚C for 20 min in electric muffle furnace

A very diminutive hump of austenite and martensite phase was observed after annealing the rolled strip at 300℃ for 20 min Both cooling and heating resulted in a one-stage shift from austenite to martensite (A→M) and from martensite to austenite (M → A). The findings suggest that the stressed-microstructure of NiTi is starting to recover after annealing. When strips of NiTi are heat treated at 350℃, a very small shift is observed in the peak position of Austenite and Martensite. At that temperature, a small hump of R-phase is observed during heating. High stress fields were responsible for inducing the rhombohedral R phase.

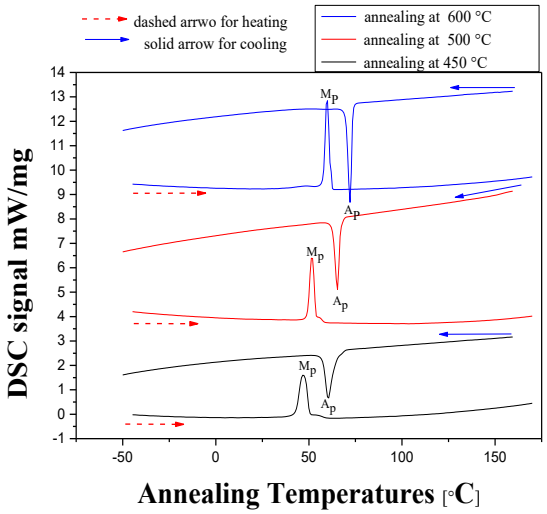

Fig. 9: DSC cooling and heating curves of the Ni-Ti alloy annealed at 450°C, 500˚C and at 600˚C for 20 min in electric muffle furnace

Annealing at 450℃, 500˚C, 600˚C a qualitative variation in phase transition behaviour

was seen when compared to all the previous DSC curves. A single parent phase structure was revealed. The Austenite and Martensite peaks are more visible. Specifically, an annealing temperature of 450°C indicates the critical temperature where the unique shift in phase behaviour was observed. Below this threshold value, transformations continued with moderate R-phase involvement, but after 450℃, the R-phase completely vanished, and the immediate martensitic transformation happened in both directions. The absence of R-phase at moderate temperatures is due to complete stress revelation.

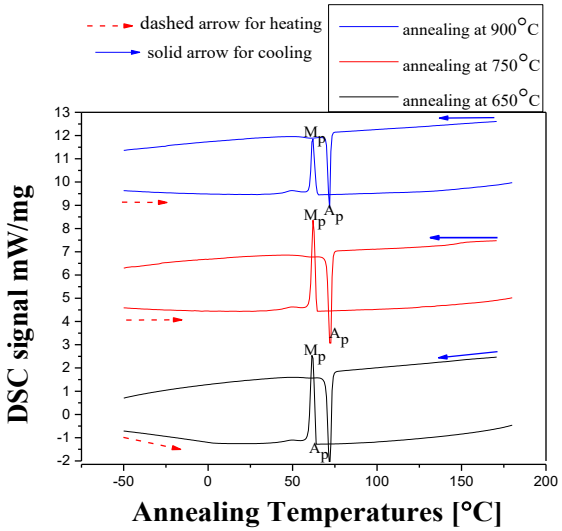

Fig. 10: DSC cooling and heating curves of the Ni-Ti alloy annealed at 650°C, 750˚C and at 900˚C for 20 min in electric muffle furnace

After annealing at 650℃, 750℃, 900℃, a qualitative variation in phase transition behaviour was seen when compared to all of the previous DSC curves. In this scenario, both cooling and heating resulted in a one-stage change from austenite to martensite (A→M) and from martensite to austenite (M→A). There is no shift found in the phase transformation of austenite and martensite peaks after that range of temperature. The R-phase is still unfound at that value of temperature. On the DSC graph, such behaviour (direct A→M phase transformation) attests to the occurrence of only one exothermic and one endothermic peak.

3.4 Thermal Cycling

Giving one DSC cycle after each experiment, no change in the transformation temperatures is observed.

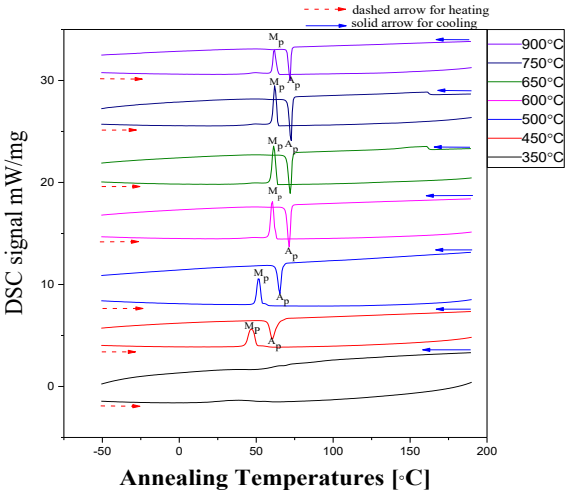

Fig. 11: All DSC cooling and heating curves of the Ni-Ti alloy after annealing at various temperatures for 20 mins in an electric muffle furnace

The transition temperatures were determined from exothermic and endothermic peaks. Positive data was collected for the heat transitions from A to R, from R to M, and from M to A, whereas negative data was collected for the heat transition from M to A. The Ms and Mf temperatures in the table are not especially accurate for as-received and annealed specimens at 300-350°C, as well as for R-phase, owing to extremely broad, flat, and indistinct DSC peaks. There was a significant shift to higher temperatures when the Ms, As, Mf, Af, and Mp, Ap temperatures were increased above 350°C, and this tendency was observed all the way up to 600°C. After 600˚C, no shift was observed in the start, finish or peak temperatures of austenite and martensite. In response to the increase in heating temperatures, the R-phase became unstable, and it ultimately vanished at 450°C, allowing for direct martensitic transformation in both directions at high temperatures.

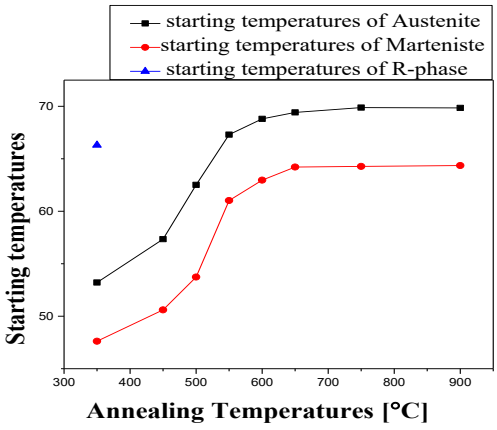

Fig. 12: Starting temperatures of austenite, martensite and R-phase

Table 2: All transformation temperatures

T [°C]	A_s	A_p	A_f	M_s	M_p	M_f	R_s	R_p	R_f
300°C	-------	53.21	-------	-------	-38.41	------	------	69.77	-------
350°C	53.21	54.71	65.36	-47.62	-40.53	-28.06	66.30	69.82	74.27
450°C	57.34	60.32	65.96	-50.60	-46.86	-43.08	------	-------	-------
500°C	62.52	65.31	67.23	-53.73	-51.70	-49.08	-------	-------	-------
550°C	67.30	70.38	71.95	-61.03	-58.77	-55.64	------	-------	-------
600°C	68.81	71.41	73.03	-62.97	-64.43	-58.13	-------	-------	-------
650°C	69.42	71.90	73.79	-64..22	-62.78	-59.22	------	-------	-------
750°C	69.88	71.95	73.79	-64.28	-62.30	-59.88	-------	-------	------
900°C	69.85	71.75	73.07	-64.36	-62.73	-59.97	------	------	-------

Table 3: All transformation temperatures of thermal cycling

T [°C]	A_s	A_p	A_f	M_s	M_p	M_f	R_s	R_p	R_f
350°C	53.21	54.71	65.36	-47.61	-40.59	-28.00	66.30	69.86	74.64
450°C	57.37	60.32	65.88	-50.60	-46.86	-43.08	------	-------	-------
500°C	62.53	65.31	67.31	-53.73	-51.70	-49.08	-------	-------	-------
550°C	67.30	70.38	71.95	-61.03	-58.77	-55.64	------	-------	-------
600°C	68.81	71.23	71.98	-62.97	-64.43	-58.13	-------	-------	-------
650°C	69.88	71.90	73.79	-64..22	-62.78	-59.22	------	-------	-------
750°C	69.85	71.38	73.94	-64.36	-61.73	-59.97	-------	-------	------

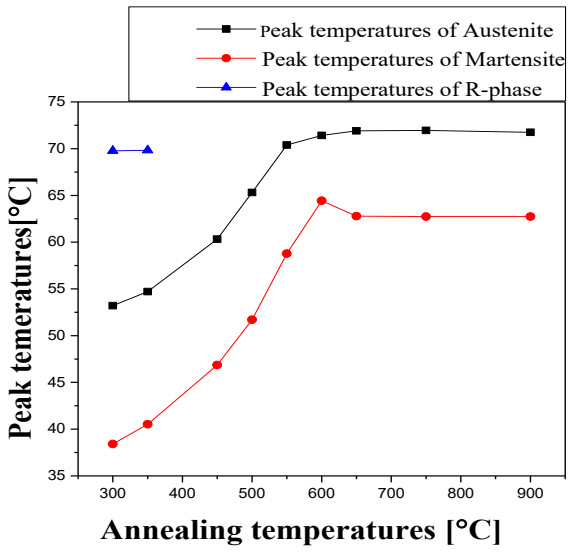

Fig. 13: Peak temperatures of austenite, martensite and R-phase

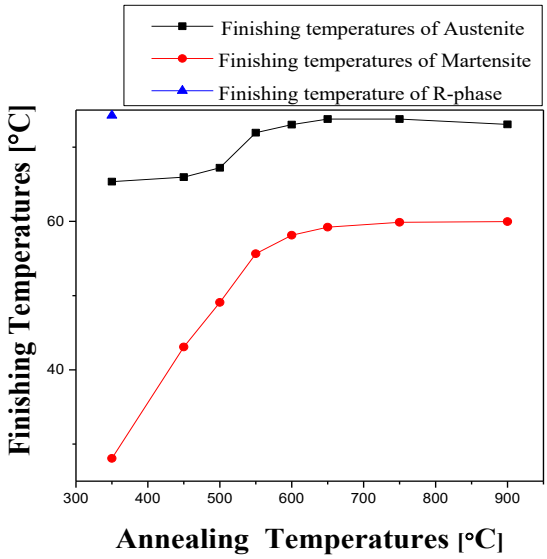

Fig. 14: Finish temperatures of austenite, martensite and R-phase

As the heat-treatment temperature was elevated, the M_p increased substantially across the temperature range, eventually reaching much higher values than had previously been seen. In this specific instance, it was discovered that the difference in temperatures between the R_p and M_p peaks was reduced gradually with increasing annealing temperature until the two exothermic peaks merged, which happened at a heat-treatment temperature of 450°C. A unique A to M and M to A transformation peak on cooling and on heating was then observed. For the A_p peak temperature, a gentle increase in the value was visible, reaching its maximum when the material was annealed at 650°C. Above this temperature, there is no rise in the peak temperatures of Austenite was found. For the material annealed at 650°C, 750˚C and 900˚C, the transformation hysteresis was about 13 ˚C approximately.

4. Conclusions

The NiTi alloy was characterized for thermal, structural, micro structure and composition analysis. From this study following conclusions can be drawn.

1. It has been revealed via XRD measurements that the alloy after intensive cold rolling includes two phases: the parent B2 phase, the martensitic B19 phase.
2. EDS analysis confirms the elemental composition of Ni and Ti (Ni= 50.14 and Ti= 49.86) in NiTi-alloy.
3. With the maximum deformation and lowest annealing temperature, the hardness of the sample is at its highest point.
4. The annealing temperature supplied to the Ni-Ti SMA in its as-received condition has proved to be an important parameter that influences the transformation mechanism and related thermal parameters.
5. Calorimetric experiments demonstrated that transformations occur in the existence of the R-phase below a specific annealing temperature. High stress fields were responsible for inducing the rhombohedral R phase.
6. 450°C was determined to be the temperature at which the single-stage phase transition of Austenite to martensite proceeds. The absence of R-phase at moderate temperatures is due to complete stress relieve.
7. The stable behaviour of transformation temperatures over a wide temperature range (650-900˚C) during annealing and thermal cycling is assumed to be due to dislocation tangling and precipitation.

5. References

[1] Van Humbeeck J. Shape memory alloys: a material and a technology. Advanced engineering materials. 2001 Nov; 3 (11):837-50.

[2] Welsch G, Boyer R, Collings EW, editors. Materials properties handbook: titanium alloys. ASM international; 1993 Dec 31.

[3] Wen C, Yu X, Zeng W, Zhao S, Wang L, Wan G, Huang S, Grover H, Chen Z. Mechanical behaviors and biomedical applications of shape memory materials: A review. AIMS Materials Science. 2018;5(4):559-90.

[4] Tarng W, Chen CJ, Lee CY, Lin CM, Lin YJ. Application of virtual reality for learning the material properties of shape memory alloys. Applied Sciences. 2019 Jan; 9 (3):580.

[5] Awan IZ, Khan AQ. Fascinating Shape Memory Alloys. Journal of the Chemical Society of Pakistan. 2018 Feb 1; 40 (1).

[6] Mahesh KK, Fernandes FB, Gurau G. Stability of thermal-induced phase transformations in the severely deformed equiatomic Ni–Ti alloys. Journal of materials science. 2012 Aug; 47 (16): 6005-14.

[7] Khademzadeh S, Parvin N, Bariani PF. Production of NiTi alloy by direct metal deposition of mechanically alloyed powder mixtures. International Journal of Precision Engineering and Manufacturing. 2015 Oct;16 (11):2333-8.

[8] Stöckel D. The shape memory effect-phenomenon, alloys and applications. California. 1995; 94539:1-3.

[9] Świec P, Zubko M, Lekston Z, Stróż D. Structure and properties of NiTi shape memory alloy after cold rolling in martensitic state.

[10] Szurman I, Kursa M. Methods for Ni-Ti based alloys preparation and their

comparison. In Proceedings of conference Metal 2010, 2010 (pp. 861-866).

[11] Pelton AR, Huang GH, Moine P, Sinclair R. Effects of thermal cycling on microstructure and properties in Nitinol. Materials Science and Engineering: A. 2012 Jan 15; 532:130-8.

[12] Kus K, Breczko T. DSC-investigations of the effect of annealing temperature on the phase transformation behaviour in Ni-Ti shape memory alloy. Materials Physics and Mechanics. 2010;9 (1):75-83.

[13] Shaw JA. Tips and tricks for characterizing shape memory alloy wire: part 1—differential scanning calorimetry and basic phenomena.

[14] Jiang SY, Zhao YN, Zhang YQ, Li HU, Liang YL. Effect of solution treatment and aging on microstructural evolution and mechanical behavior of NiTi shape memory alloy. Transactions of Nonferrous Metals Society of China. 2013 Dec 1; 23 (12): 36.

[15] Uchil J, Mohanchandra KP, Mahesh KK, Kumara KG. Thermal and electrical characterization of R-phase dependence on heat-treat temperature in Nitinol. Physica B: Condensed Matter. 1998 Oct 1; 253 (1-2): 83-9.